Lyapunov exponent calculation of a two-degree-of-freedom vibro-impact system with symmetrical rigid stops*

Li Qun-Hong(李群宏)† and Tan Jie-Yan(谭洁燕)

College of Mathematics and Information Science, Guangxi University, Nanning 530004, *China*

(Received 14 August 2010; revised manuscript received 16 November 2010)

A two-degree-of-freedom vibro-impact system having symmetrical rigid stops and subjected to periodic excitation is investigated in this paper. By introducing local maps between different stages of motion in the whole impact process, the Poincaré map of the system is constructed. Using the Poincaré map and the Gram–Schmidt orthonormalization, a method of calculating the spectrum of Lyapunov exponents of the above vibro-impact system is presented. Then the phase portraits of periodic and chaotic attractors for the system and the corresponding convergence diagrams of the spectrum of Lyapunov exponents are given out through the numerical simulations. To further identify the validity of the aforementioned computation method, the bifurcation diagram of the system with respect to the bifurcation parameter and the corresponding largest Lyapunov exponents are shown.

Keywords: vibro-impact system, Poincaré map, Gram–Schmidt orthonormalization, Lyapunov exponent

PACS: 05.45.–a, 05.10.–a **DOI:** 10.1088/1674-1056/20/4/040505

1. Introduction

In the investigation of nonlinear non-smooth vibro-impact systems, the spectrum of Lyapunov exponents plays an important role in determining the dynamic characteristics. Also, it is an exponential measure of average divergence or convergence of nearby orbits in the phase space.

There have been many results for calculating the spectrum of Lyapunov exponents of smooth dynamical systems described by differential equations and discrete mapping systems.[1,2] Wolf *et al.*[3] presented the first algorithms to estimate the non-negative Lyapunov exponents from an experimental time series. However, for the non-smooth systems, the Jacobian matrices make no sense at non-smooth points so that it is more difficult to calculate the spectrum of Lyapunov exponents of non-smooth systems.

In recent years, some research has been done on the computation methods of the spectrum of Lyapunov exponents. Müller[4] added certain transitional conditions to the linearized equations at the instants of impacts and applied the classical calculation methods of Lyapunov exponents to non-smooth systems. de Souza and Caldas[5] considered a model based algorithm for the calculation of the spectrum of the Lyapunov exponents of attractors of mechanical systems with impacts. To implement this algorithm they introduced a transcendental map that described the solutions of the integrable differential equations, between impacts, supplemented with transition conditions at the instants of impacts. Hence, the classical calculation methods for the spectrum of Lyapunov exponents of smooth dynamical systems could be applied to non-smooth systems in this case. Nordmark[6] analysed the grazing bifurcation by means of the local maps. In particular, the derivative formula of the switch map was given in Nordmark's paper. Using the local map, Jin and Lu[7] constructed the Poincaré map for the whole impact process to avoid the problem of defining the Jacobian matrices at non-smooth points. Then according to the method of calculating the spectrum of Lyapunov exponents of discrete-time smooth system, they presented a more general method of calculating the spectrum of Lyapunov exponents of n-dimensional non-smooth dynamical systems. In addition, Luo *et al.*[8] calculated the Lyapunov exponents

*Project supported by the National Natural Science Foundation of China (Grant No. 10972059), the Natural Science Foundation of the Guangxi Zhuang Autonmous Region of China (Grant Nos. 0640002 and 2010GXNSFA013110), the Guangxi Youth Science Foundation of China (Grant No. 0832014) and the Project of Excellent Innovating Team of Guangxi University.

†Corresponding author. E-mail: liqh@gxu.edu.cn

© 2011 Chinese Physical Society and IOP Publishing Ltd

of a two-degree-of-freedom vibro-impact system with symmetrical rigid stops via the transcendental impact map. Yue and Xie[9] considered a vibro-impact system with symmetric two-sided rigid constraints in which the six-dimensional Poincaré map can be expressed as the second iteration of another unsymmetric implicit map. Based on the QR method, the unsymmetric implicit map was used to calculate all the Lyapunov exponents. Stefanski[10] investigated the largest Lyapunov exponent for mechanical systems with impact using the properties of synchronization phenomenon. Liu *et al.*[11] studied the global vector-field reconstruction of nonlinear dynamical systems from a time series. Lyapunov exponents and dimension, calculated from the differential equations of a standard system, were used for the validation of the reconstruction.

In this paper, we give a further development of the Lyapunov exponent computing method in Ref. [7]. Compared with Ref. [7] which focused on the systems with unilateral constraint, this paper deals with a two-degree-of-freedom vibro-impact system with bilateral constraints, which possesses the different construction of the Poincaré map from that of Ref. [7] because the presence of two-sided stops leads to the complexity of the Poincaré map. Since there exist many dynamical systems with several constraints in the engineering fields, it is worth while discussing the calculation of Lyapunov exponents of these systems so that the complicated dynamics of systems with several constraints can be obtained.

2. Mechanical model and equations of motion

A two-degree-of-freedom system having symmetrically placed rigid stops and subjected to periodic excitation is shown in Fig. 1. Displacements of the masses M_1 and M_2 are represented by X_1 and X_2, respectively. The masses are connected to linear springs with stiffnesses K_1 and K_2 and linear viscous dashpots with damping constants C_1 and C_2. The masses move only in the horizontal direction. The excitations on both masses are harmonic and take the forms of $P_i \sin(\Omega T + \tau)$, $(i = 1, 2)$. When the displacement X_1 of the mass M_1 is B (or $-B$), the mass M_1 will hit the rigid stop A (or C) and the velocity of the mass M_1 will change its value and direction. Thus M_1 may hit the stop C (or A) in the consequent moving. The other mass M_2 is not allowed to impact any rigid stop during the whole motion. M_1 moves between rigid stops A and C and hits the stops again and again. Damping in the mechanical model is assumed to be proportional damping of the Rayleigh type, which in this case implies $C_1/K_1 = C_2/K_2$. The impact is described by a coefficient of restitution R and it is assumed that the duration of impact is negligible compared with the period of the force.

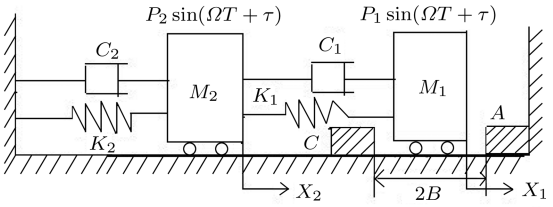


Fig. 1. Schematic representation of a two-degree-of-freedom vibro-impact system with symmetrical rigid stops.

Between any two consecutive impacts ($|X_1| < B$), the differential equations of motion are given by

$$\begin{bmatrix} M_1 & 0 \\ 0 & M_2 \end{bmatrix} \begin{Bmatrix} \ddot{X}_1 \\ \ddot{X}_2 \end{Bmatrix} + \begin{bmatrix} C_1 & -C_1 \\ -C_1 & C_1 + C_2 \end{bmatrix} \begin{Bmatrix} \dot{X}_1 \\ \dot{X}_2 \end{Bmatrix} + \begin{bmatrix} K_1 & -K_1 \\ -K_1 & K_1 + K_2 \end{bmatrix} \begin{Bmatrix} X_1 \\ X_2 \end{Bmatrix} = \begin{bmatrix} P_1 \\ P_2 \end{bmatrix} \sin(\Omega T + \tau), \quad |X_1| < B. \tag{1}$$

The impacting equations of mass M_1 can be written as

$$\begin{aligned} \dot{X}_{1A+} &= -R\dot{X}_{1A-}, \quad (X_1 = B), \\ \dot{X}_{1C+} &= -R\dot{X}_{1C-}, \quad (X_1 = -B), \end{aligned} \tag{2}$$

where the subscripts $-, +$ denote the values before and after impact, respectively.

Introduce the following dimensionless quantities:

$$\begin{aligned} &\mu_m = \frac{M_2}{M_1}, \quad \mu_k = \frac{K_2}{K_1}, \quad \mu_c = \frac{C_2}{C_1} = \mu_k, \\ &f_2 = \frac{P_2}{P_1 + P_2}, \quad \omega = \Omega \sqrt{\frac{M_1}{K_1}}, \\ &t = T\sqrt{\frac{K_1}{M_1}}, \quad \zeta = \frac{C_2}{2\sqrt{K_1 M_1}}, \\ &b = \frac{BK_1}{P_1 + P_2}, \quad x_i = \frac{X_i K_1}{P_1 + P_2}, \end{aligned}$$

then the dimensionless differential equations of motion without impacting will become

$$\begin{bmatrix} 1 & 0 \\ 0 & \mu_m \end{bmatrix} \begin{Bmatrix} \ddot{x}_1 \\ \ddot{x}_2 \end{Bmatrix} + \begin{bmatrix} 2\zeta & -2\zeta \\ -2\zeta & 2\zeta(1 + \mu_c) \end{bmatrix} \begin{Bmatrix} \dot{x}_1 \\ \dot{x}_2 \end{Bmatrix}$$

$$+\begin{bmatrix} 1 & -1 \\ -1 & 1+\mu_k \end{bmatrix}\begin{Bmatrix} x_1 \\ x_2 \end{Bmatrix} = \begin{bmatrix} 1-f_2 \\ f_2 \end{bmatrix}\sin(\omega t+\tau), \quad |x_1|<b, \tag{3}$$

and the impacting equations of mass M_1 will be

$$\begin{aligned} \dot{x}_{1A+} &= -R\dot{x}_{1A-}, \quad (x_1 = b), \\ \dot{x}_{1C+} &= -R\dot{x}_{1C-}, \quad (x_1 = -b). \end{aligned} \tag{4}$$

Let Ψ represent the canonical modal matrix of Eq. (3), ω_1 and ω_2 denote the eigenfrequencies of the system as impacts do not occur. Taking Ψ as a transition matrix, the equation of motion (3), under the transform of variables $X = \Psi\xi$, becomes

$$I\ddot{\xi} + C\dot{\xi} + \Lambda\xi = \bar{F}\sin(\omega t+\tau), \tag{5}$$

where $X = (x_1, x_2)^{\mathrm{T}}$, $\xi = (\xi_1, \xi_2)^{\mathrm{T}}$, I is a 2×2 unit matrix, C and Λ are diagonal matrices, and $C = \mathrm{diag}[\,2\zeta\omega_1^2, 2\zeta\omega_2^2\,]$, $\Lambda = \mathrm{diag}[\,\omega_1^2, \omega_2^2\,]$, $\bar{F} = (\bar{f}_1, \bar{f}_2)^{\mathrm{T}} = \Psi^{\mathrm{T}}P_k$, $P_k = (1-f_2, f_2)^{\mathrm{T}}$. The equations of motion (3) are solved by using the modal co-ordinates and the modal matrix approach. The general solution takes the form

$$\begin{aligned} x_i(t) = \sum_{j=1}^{2}\psi_{ij}\big(\,&\mathrm{e}^{-\eta_j(t-t_0)}(a_{j1}\cos\omega_{dj}(t-t_0) \\ &+ b_{j1}\sin\omega_{dj}(t-t_0)) + A_j\sin(\omega t+\tau) \\ &+ B_j\cos(\omega t+\tau)\big), \ t_0 \le t \le t_1, \\ x_i(t) = \sum_{j=1}^{2}\psi_{ij}\big(\,&\mathrm{e}^{-\eta_j(t-t_1)}(a_{j2}\cos\omega_{dj}(t-t_1) \\ &+ b_{j2}\sin\omega_{dj}(t-t_1)) + A_j\sin(\omega t+\tau) \\ &+ B_j\cos(\omega t+\tau)\big), \ t_1 \le t \le t_2, \end{aligned} \tag{6}$$

where it takes the time $t_1 - t_0$ and $t_2 - t_1$, respectively, for the mass M_1 to move from the constraint A to C and from the constraint C to A, ψ_{ij} are the elements of the canonical modal matrix Ψ, $\eta_j = \zeta\omega_j^2$, $\omega_{dj} = \sqrt{\omega_j^2 - \eta_j^2}$, a_{jk} and b_{jk} $(k = 1, 2)$ are the constants of integration which are determined by the initial condition and modal parameters of the system. A_j and B_j are the amplitude parameters, which are given as

$$A_j = \frac{1}{2\omega_{dj}}\left(\frac{\omega+\omega_{dj}}{(\omega+\omega_{dj})^2+\eta_j^2} - \frac{\omega-\omega_{dj}}{(\omega-\omega_{dj})^2+\eta_j^2}\right)\bar{f}_j, \tag{7}$$

$$B_j = \frac{\eta_j}{2\omega_{dj}}\left(\frac{1}{(\omega+\omega_{dj})^2+\eta_j^2} - \frac{1}{(\omega-\omega_{dj})^2+\eta_j^2}\right)\bar{f}_j. \tag{8}$$

Let $\dot{x}_1 = v_1$, $\dot{x}_2 = v_2$ and $\varphi = \omega t$, $(\mathrm{mod}2\pi)$, then equation (5) can be changed into one-order autonomous dynamical system

$$\begin{pmatrix} \dot{x}_1 \\ \dot{v}_1 \\ \dot{x}_2 \\ \dot{v}_2 \\ \dot{\varphi} \end{pmatrix} = \begin{pmatrix} v_1 \\ -2\zeta v_1 + 2\zeta v_2 - x_1 + x_2 + (1-f_2)\sin(\varphi+\tau) \\ v_2 \\ \dfrac{2\zeta v_1 - 2\zeta(1+\mu_c)v_2 + x_1 - (1+\mu_k)x_2 + f_2\sin(\varphi+\tau)}{\mu_m} \\ \omega \end{pmatrix}, \tag{9}$$

where the analytical expressions of x_i and v_i $(i = 1, 2)$ can be obtained by Eq. (6).

3. Poincaré map of the vibro-impact system and its Jacobian matrix

For convenience of description, we assume that the oscillator M_1 collides with each stop only once at every one period of the external excitation. Here the constant phase surface Π^{φ} before impact is taken as the Poincaré section, that is,

$$\begin{aligned} \Pi^{\varphi_A} &= \{(x_1, v_1, x_2, v_2, \varphi) \\ &\in R^4\times S^1 | \varphi - \varphi_A = 0\}, \end{aligned} \tag{10}$$

$$\begin{aligned} \Pi^{\varphi_C} &= \{(x_1, v_1, x_2, v_2, \varphi) \\ &\in R^4\times S^1 | \varphi - \varphi_C = 0\}. \end{aligned} \tag{11}$$

Construct the Poincaré map

$$P = P_C \circ P_A, \tag{12}$$

where $P_A : \Pi^{\varphi_A} \to \Pi^{\varphi_C}, P_C : \Pi^{\varphi_C} \to \Pi^{\varphi_A}$ and the impact surfaces Σ_A and Σ_C are defined as

$$\Sigma_A = \{(x_1, v_1, x_2, v_2, \varphi) \in R^4\times S^1 | x_1 = b\}, \tag{13}$$

$$\Sigma_C = \{(x_1, v_1, x_2, v_2, \varphi) \in R^4 \times S^1 | x_1 = -b\}. \quad (14)$$

The Poincaré map P is constructed as Eq. (12). Figure 2 shows the scenario of a trajectory crossing the Poincaré section in the state space.

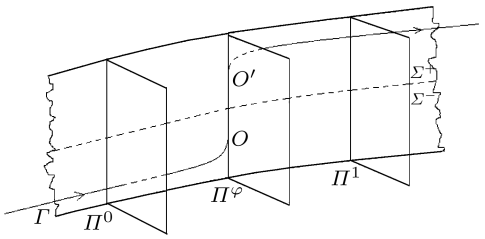


Fig. 2. A trajectory crosses the Poincaré section.

Suppose that O $(O') \in \Pi^{\varphi} \cap \Sigma$. If a trajectory in the neighbourhood of O (O') crosses from the constant phase surface Π^{φ} to the switch section Σ (or from the impact section Σ to the switch surface Π^{φ}), the corresponding map is said to be a local map.

Let $z = (x, \varphi)^{\mathrm{T}} \in R^4 \times S^1$ and $F(z) = (f(z), \omega)^{\mathrm{T}}$ be the vector field in the state space $R^4 \times S^1$, let $h(z) = 0$ be the equation of the switch surface and define a local map P^{L}, then the Jacobian matrix of P^{L} near the point $O(z_0)$ can be denoted as[6]

$$DP^{\mathrm{L}}(z_0) = I - \frac{F(z_0)Dh(z_0)}{Dh(z_0) \cdot F(z_0)}, \quad (15)$$

where I is a 5×5 unit matrix.

According to the situation of the trajectory intersecting with the impact section Σ, four kinds of maps are defined: (i) a local map P_1 from the constant phase section Π^{φ} near the point O to the impact section Σ^-; (ii) an impact map P_2 from the impact section Σ^- near the point O to the impact section Σ^+ near the point O'; (iii) a local map P_3 from the impact section Σ^+ to the constant phase section Π^{φ} near the point O'; (iv) a flow map from the constant phase section Π^{φ} to the next constant phase section Π^{φ} in the non-impact process.

Let

$$\begin{aligned} &P_{1A} : \Pi^{\varphi_A} \to \Sigma_A^-, \quad P_{2A} : \Sigma_A^- \to \Sigma_A^+, \\ &P_{3A} : \Sigma_A^+ \to \Pi^{\varphi_A}, \quad P_{4A} : \Pi^{\varphi_A} \to \Pi^{\varphi_C}, \\ &P_{1C} : \Pi^{\varphi_C} \to \Sigma_C^-, \quad P_{2C} : \Sigma_C^- \to \Sigma_C^+, \\ &P_{3C} : \Sigma_C^+ \to \Pi^{\varphi_C}, \quad P_{4C} : \Pi^{\varphi_C} \to \Pi^{\varphi_A}. \end{aligned} \quad (16)$$

Now consider the above eight maps with their Jacobian matrices in detail. We use $(x_{1A-}, v_{1A-}, x_{2A-}, v_{2A-}, \varphi_{A-})$ and $(x_{1A+}, v_{1A+}, x_{2A+}, v_{2A+}, \varphi_{A+})$ to denote the instants before and after the impacts on the impact section Σ_A, respectively. It is an instant impact and the mass M_2 is not allowed to impact any rigid stops, so $x_{1A-} = x_{1A+}$, $x_{2A-} = x_{2A+}$, $v_{2A-} = v_{2A+}$, $\varphi_{A-} = \varphi_{A+}$.

(I) Map P_{1A} and its Jacobian matrix

The map P_{1A} denotes a local map that makes the trajectory cross from the constant phase section Π^{φ_A} to the impact section Σ_A^-, that is,

$$\begin{aligned} &P_{1A} : \Pi^{\varphi_A} \to \Sigma_A^-, \\ &(x_{1\varphi_A}, v_{1\varphi_A}, x_{2\varphi_A}, v_{2\varphi_A})^{\mathrm{T}} \\ \mapsto\ &(v_{1A-}, x_{2A-}, v_{2A-}, \varphi_{A-})^{\mathrm{T}}. \end{aligned} \quad (17)$$

Here the switch surface Σ_A^- is the impact section and its equation is $h(z_A) = x_1 - b = 0$. The Jacobian matrix of the local map P_{1A} can be calculated by Eq. (15) and vector field (9) as follows:

$$DP_{1A} = \begin{pmatrix} a_{11} & 1 & 0 & 0 \\ -\dfrac{v_{2A-}}{v_{1A-}} & 0 & 1 & 0 \\ a_{31} & 0 & 0 & 1 \\ -\dfrac{\omega}{v_{1A-}} & 0 & 0 & 0 \end{pmatrix}, \quad (18)$$

where $a_{11} = (2\zeta v_{1A-} - 2\zeta v_{2A-} + x_{1A-} - x_{2A-} - (1 - f_2)\sin(\varphi_{A-} + \tau))/v_{1A-}$ and $a_{31} = (-2\zeta v_{1A-} + 2\zeta(1+\mu_c)v_{2A-} - x_{1A-} + (1+\mu_k)x_{2A-} - f_2 \sin(\varphi_{A-} + \tau))/\mu_m v_{1A-}$.

(II) Map P_{2A} and its Jacobian matrix

The map P_{2A} denotes an impact map from the impact section Σ_A^- to the impact section Σ_A^+, that is,

$$\begin{aligned} &P_{2A} : \Sigma_A^- \to \Sigma_A^+, \\ &(v_{1A-}, x_{2A-}, v_{2A-}, \varphi_{A-})^{\mathrm{T}} \\ \mapsto\ &(v_{1A+}, x_{2A+}, v_{2A+}, \varphi_{A+})^{\mathrm{T}}. \end{aligned} \quad (19)$$

The Jacobian matrix of the map P_{2A} can be given by the instantaneous velocity property of mass M_1 as

$$DP_{2A} = \begin{pmatrix} -R & 0 & 0 & 0 \\ 0 & 1 & 0 & 0 \\ 0 & 0 & 1 & 0 \\ 0 & 0 & 0 & 1 \end{pmatrix}. \quad (20)$$

(III) Map P_{3A} and its Jacobian matrix

The map P_{3A} denotes a local map from the impact section Σ_A^+ to the constant phase section Π^{φ_A}, that is,

$$\begin{aligned} &P_{3A} : \Sigma_A^+ \to \Pi^{\varphi_A}, \\ &(v_{1A+}, x_{2A+}, v_{2A+}, \varphi_{A+})^{\mathrm{T}} \\ \mapsto\ &(x_{1\varphi_A}, v_{1\varphi_A}, x_{2\varphi_A}, v_{2\varphi_A})^{\mathrm{T}}. \end{aligned} \quad (21)$$

Here the equation of the switch surface is $h(z_A) = \varphi - \varphi_A = 0$. The Jacobian matrix of the local map P_{3A} can be calculated by Eq. (15) and vector field (9) as follows:

$$DP_{3A} = \begin{pmatrix} 0 & 0 & 0 & -\dfrac{v_{1A+}}{\omega} \\ 1 & 0 & 0 & a_{24} \\ 0 & 1 & 0 & -\dfrac{v_{2A+}}{\omega} \\ 0 & 0 & 1 & a_{44} \end{pmatrix}, \tag{22}$$

where $a_{24} = (2\zeta v_{1A+} - 2\zeta v_{2A+} + x_{1A+} - x_{2A+} - (1 - f_2)\sin(\varphi_{A+} + \tau))/\omega$ and $a_{44} = (-2\zeta v_{1A+} + 2\zeta(1 + \mu_c)v_{2A+} - x_{1A+} + (1+\mu_k)x_{2A+} - f_2\sin(\varphi_{A+}+\tau))/\mu_m\omega$.

(IV) Map P_{4A} and its Jacobian matrix

The map P_{4A} denotes a flow map that makes the trajectory cross from the constant phase section Π^{φ_A} to the constant phase section Π^{φ_C}, that is,

$$\begin{aligned} & P_{4A} : \Pi^{\varphi_A} \to \Pi^{\varphi_C}, \\ & (x_{1\varphi_A}, v_{1\varphi_A}, x_{2\varphi_A}, v_{2\varphi_A})^{\mathrm{T}} \\ \mapsto \quad & (x_{1\varphi_C}, v_{1\varphi_C}, x_{2\varphi_C}, v_{2\varphi_C})^{\mathrm{T}}. \end{aligned} \tag{23}$$

In this non-impact process, no trajectory goes through the impact section. Thus, its Jacobian matrix can be obtained by the differentiation rule of multivariate functions and Eq. (6).

Let $(x_{1C-}, v_{1C-}, x_{2C-}, v_{2C-}, \varphi_{C-})$ and $(x_{1C+}, v_{1C+}, x_{2C+}, v_{2C+}, \varphi_{C+})$ be the instants before and after impacts on the impact section Σ_C, respectively. It is an instant impact and the mass M_2 is not allowed to impact any rigid stops, so $x_{1C-} = x_{1C+}$, $x_{2C-} = x_{2C+}$, $v_{2C-} = v_{2C+}$, $\varphi_{C-} = \varphi_{C+}$.

(V) Map P_{1C} and its Jacobian matrix

The map P_{1C} denotes a local map from the constant phase section Π^{φ_C} to the impact section Σ_C^-,

$$\begin{aligned} & P_{1C} : \Pi^{\varphi_C} \to \Sigma_C^-, \\ & (x_{1\varphi_C}, v_{1\varphi_C}, x_{2\varphi_C}, v_{2\varphi_C})^{\mathrm{T}} \\ \mapsto \quad & (v_{1C-}, x_{2C-}, v_{2C-}, \varphi_{C-})^{\mathrm{T}}, \end{aligned} \tag{24}$$

where the switch surface is the impact section Σ_C^- and its equation is $h(z_C) = x_1 + b = 0$. The Jacobian matrix of the local map P_{1C} can be calculated by Eq. (15) and vector field (9) as follows:

$$DP_{1C} = \begin{pmatrix} c_{11} & 1 & 0 & 0 \\ -\dfrac{v_{2C-}}{v_{1C-}} & 0 & 1 & 0 \\ c_{31} & 0 & 0 & 1 \\ -\dfrac{\omega}{v_{1C-}} & 0 & 0 & 0 \end{pmatrix}, \tag{25}$$

where $c_{11} = (2\zeta v_{1C-} - 2\zeta v_{2C-} + x_{1C-} - x_{2C-} - (1 - f_2)\sin(\varphi_{C-} + \tau))/v_{1C-}$ and $c_{31} = (-2\zeta v_{1C-} + 2\zeta(1+\mu_c)v_{2C-} - x_{1C-} + (1+\mu_k)x_{2C-} - f_2\sin(\varphi_{C-} + \tau))/\mu_m v_{1C-}$.

(VI) Map P_{2C} and its Jacobian matrix

The map P_{2C} denotes an impact map from the impact section Σ_C^- to the impact section Σ_C^+, that is,

$$\begin{aligned} & P_{2C} : \Sigma_C^- \to \Sigma_C^+, \\ & (v_{1C-}, x_{2C-}, v_{2C-}, \varphi_{C-})^{\mathrm{T}} \\ \mapsto \quad & (v_{1C+}, x_{2C+}, v_{2C+}, \varphi_{C+})^{\mathrm{T}}. \end{aligned} \tag{26}$$

The Jacobian matrix of the map P_{2C} can be given by the instantaneous velocity property of mass M_1 as

$$DP_{2C} = \begin{pmatrix} -R & 0 & 0 & 0 \\ 0 & 1 & 0 & 0 \\ 0 & 0 & 1 & 0 \\ 0 & 0 & 0 & 1 \end{pmatrix}. \tag{27}$$

(VII) Map P_{3C} and its Jacobian matrix

The P_{3C} denotes a local map from the impact section Σ_C^+ to the constant phase section Π^{φ_C}, that is,

$$\begin{aligned} & P_{3C} : \Sigma_C^+ \to \Pi^{\varphi_C}, \\ & (v_{1C+}, x_{2C+}, v_{2C+}, \varphi_{C+})^{\mathrm{T}} \\ \mapsto \quad & (x_{1\varphi_C}, v_{1\varphi_C}, x_{2\varphi_C}, v_{2\varphi_C})^{\mathrm{T}}, \end{aligned} \tag{28}$$

where the equation of the switch surface is $h(z_C) = \varphi - \varphi_C = 0$. The Jacobian matrix of the local map P_{3C} can be calculated by Eq. (15) and the vector field (9) as follows:

$$DP_{3C} = \begin{pmatrix} 0 & 0 & 0 & -\dfrac{v_{1C+}}{\omega} \\ 1 & 0 & 0 & c_{24} \\ 0 & 1 & 0 & -\dfrac{v_{2C+}}{\omega} \\ 0 & 0 & 1 & c_{44} \end{pmatrix}, \tag{29}$$

where $c_{24} = (2\zeta v_{1C+} - 2\zeta v_{2C+} + x_{1C+} - x_{2C+} - (1 - f_2)\sin(\varphi_{C+} + \tau))/\omega$ and $c_{44} = (-2\zeta v_{1C+} + 2\zeta(1 + \mu_c)v_{2C+} - x_{1C+} + (1+\mu_k)x_{2C+} - f_2\sin(\varphi_{C+}+\tau))/\mu_m\omega$.

(VIII) Map P_{4C} and its Jacobian matrix

The map P_{4C} denotes a flow map that makes the trajectory cross from the constant phase section Π^{φ_C} to the constant phase section Π^{φ_A}, that is,

$$\begin{aligned} & P_{4C} : \Pi^{\varphi_C} \to \Pi^{\varphi_A}, \\ & (x_{1\varphi_C}, v_{1\varphi_C}, x_{2\varphi_C}, v_{2\varphi_C})^{\mathrm{T}} \\ \mapsto \quad & (x_{1\varphi_A}, v_{1\varphi_A}, x_{2\varphi_A}, v_{2\varphi_A})^{\mathrm{T}}. \end{aligned} \tag{30}$$

Just as we said before, it is a non-impact process, no trajectory goes through the impact section. Its Jacobian matrix can be obtained by the differentiation rule of multivariate functions and Eq. (6).

Since system (9) contains several nonlinear equations with respect to x_1, v_1, x_2 and v_2. Thus it is difficult to obtain analytic expressions of the entries of matrices DP_{4A} and DP_{4C}. Let $X = (x_1, v_1, x_2, v_2)^{\mathrm{T}}$, then

$$DP_{4A} = \left.\frac{\partial X}{\partial X_{\varphi_{A+}}}\right|_{\varphi=\varphi_{C-}},$$
$$DP_{4C} = \left.\frac{\partial X}{\partial X_{\varphi_{C+}}}\right|_{\varphi=\varphi_{A-}}. \tag{31}$$

The numerical solutions of DP_{4A} and DP_{4C} can be obtained by solving the following initial value problems:

$$\begin{cases} \dfrac{\mathrm{d}}{\mathrm{d}t}\left[\dfrac{\partial X}{\partial X_{\varphi_{A+}}}\right] = \dfrac{\partial f}{\partial X}\dfrac{\partial X}{\partial X_{\varphi_{A+}}}, \\ \left.\dfrac{\partial X}{\partial X_{\varphi_{A+}}}\right|_{\varphi=\varphi_{A+}} = I, \end{cases}$$
$$\begin{cases} \dfrac{\mathrm{d}}{\mathrm{d}t}\left[\dfrac{\partial X}{\partial X_{\varphi_{C+}}}\right] = \dfrac{\partial f}{\partial X}\dfrac{\partial X}{\partial X_{\varphi_{C+}}}, \\ \left.\dfrac{\partial X}{\partial X_{\varphi_{C+}}}\right|_{\varphi=\varphi_{C+}} = I, \end{cases} \tag{32}$$

where f represents the vector field of system (9) and I is the four-dimensional identical matrix.

The Jacobian matrix of the Poincaré map can be obtained by the derivation chain rule of the compound function, that is,

$$DP_A = DP_{4A} \circ DP_{3A} \circ DP_{2A} \circ DP_{1A},$$
$$DP_C = DP_{4C} \circ DP_{3C} \circ DP_{2C} \circ DP_{1C}. \tag{33}$$

If the mass M_1 impacts both rigid stops m times in one external excitation period, we can obtain the Poincaré map by compounding m former maps, that is,

$$P = P_4 \circ (P_C \circ P_A)^m, \tag{34}$$

where P_4 is a smooth flow map mapping the orbit onto the constant phase section. If after m impacts on both impact surfaces, the orbit is just on the constant phase section exactly, then P_4 is an identity map. In this case, the Jacobian matrix of map P can be written as

$$DP = DP_4 \circ (DP_C \circ DP_A)^m. \tag{35}$$

Notice that here the Poincaré map for motions contacting with symmetrical rigid stops has been described. If unilateral collision is involved in the motion, the corresponding Poincaré map can be derived in a way similar to that in the above discussion.

4. Calculation of the spectrum of Lyapunov exponents of vibo-impact system

As shown before, the Poincaré map method is adopted using the Poincaré map P given in Eq. (12):

$$x^{(k)} = P(x^{(k-1)}), \quad x^{(k-1)} \in \Pi^{\varphi},\ k \in \boldsymbol{Z}. \tag{36}$$

On the constant phase section Π^{φ}, one chooses two nearby points $x^{(0)}$ and $x^{(0)} + \delta x^{(0)}$, from which originate the nearby orbits G_1 and G_2 of discrete dynamical system (36). At the time of $(k-1)$, the points on the basis orbit and the nearby orbit are denoted as $x^{(k-1)}(x^{(0)})$ and $x^{(k-1)}(x^{(0)} + \delta x^{(0)})$, respectively.

Let $\delta x^{(k-1)}(x^{(0)}) = x^{(k-1)}(x^{(0)} + \delta x^{(0)}) - x^{(k-1)}(x^{(0)})$. When $\delta x^{(k-1)}$ is sufficiently small, the linearized equation of system (36) at the point $x^{(0)}$ is given as follows:

$$\delta x^{(k)} = DP(x^{(k-1)}) \cdot \delta x^{(k-1)}, \tag{37}$$

where $DP(x^{(k-1)})$ is the 4×4 Jacobian matrix of Eq. (36) at the point $x^{(k-1)}$.

From formulae (36) and (37), it follows that

$$\delta x^{(k)} = DP^k(x^{(0)}) \cdot \delta x^{(0)}, \tag{38}$$

where $DP^k(x^{(0)}) = DP(x^{(k-1)}) \cdot DP(x^{(k-2)}) \cdots DP(x^{(0)})$.

In order to compute the spectrum of Lyapunov exponents, we compute the average exponent divergence rate between the basis orbit beginning at the point $x^{(0)}$ and its nearby orbit along the direction of $u^{(0)} = \delta x^{(0)} / \parallel \delta x^{(0)} \parallel$ by the following formula:

$$\lambda(x^{(0)}, u^{(0)}) = \lim_{k\to\infty} \frac{1}{k} \ln \frac{\parallel \delta x^{(k)} \parallel}{\parallel \delta x^{(0)} \parallel}, \tag{39}$$

where $\parallel \delta x^{(k)} \parallel$ is the norm of $\delta x^{(k)}$, $(k = 0, 1, 2, \ldots)$.

Next we will discuss the calculation of the spectrum of Lyapunov exponents of Eq. (9). One can choose four linearly independent perturbations $(\delta x_1^{(0)}, \delta x_2^{(0)}, \delta x_3^{(0)}, \delta x_4^{(0)})$ and define the vector

$$\left(u_1^{(0)}, u_2^{(0)}, u_3^{(0)}, u_4^{(0)}\right) = \left(\frac{\delta x_1^{(0)}}{\parallel \delta x_1^{(0)} \parallel}, \frac{\delta x_2^{(0)}}{\parallel \delta x_2^{(0)} \parallel}, \frac{\delta x_3^{(0)}}{\parallel \delta x_3^{(0)} \parallel}, \frac{\delta x_4^{(0)}}{\parallel \delta x_4^{(0)} \parallel}\right). \tag{40}$$

Then, taking $(u_1^{(0)}, u_2^{(0)}, u_3^{(0)}, u_4^{(0)})$ as the initial vector and according to Eqs. (33) and (35), we

obtain the vector $(\delta x_1^{(1)}, \delta x_2^{(1)}, \delta x_3^{(1)}, \delta x_4^{(1)})$. Applying the Gram–Schmidt orthonormalization to the vector $(\delta x_1^{(1)}, \delta x_2^{(1)}, \delta x_3^{(1)}, \delta x_4^{(1)})$, the vector $(u_1^{(1)}, u_2^{(1)}, u_3^{(1)}, u_4^{(1)})$ is obtained, which will be used as the initial value of the next iteration. The result of Gram–Schmidt orthonormalization can be described as follows:

$$\begin{cases} m_1^{(n)} = \delta x_1^{(n)}, \\ u_1^{(n)} = m_1^{(n)} / \parallel m_1^{(n)} \parallel, \\ m_2^{(n)} = \delta x_2^{(n)} - \langle \delta x_2^{(n)},\ u_1^{(n)} \rangle u_1^{(n)}, \\ u_2^{(n)} = m_2^{(n)} / \parallel m_2^{(n)} \parallel, \\ m_3^{(n)} = \delta x_3^{(n)} - \langle \delta x_3^{(n)}, u_1^{(n)} \rangle u_1^{(n)} \\ \qquad -\langle \delta x_3^{(n)}, u_2^{(n)} \rangle\ u_2^{(n)}, \\ u_3^{(n)} = m_3^{(n)} / \parallel m_3^{(n)} \parallel, \\ m_4^{(n)} = \delta x_4^{(n)} - \langle \delta x_4^{(n)}, u_1^{(n)} \rangle u_1^{(n)} \\ \qquad -\langle \delta x_4^{(n)}, u_2^{(n)} \rangle u_2^{(n)} - \langle \delta x_4^{(n)}, u_3^{(n)} \rangle\ u_3^{(n)}, \\ u_4^{(n)} = m_4^{(n)} / \parallel m_4^{(n)} \parallel, \end{cases} \tag{41}$$

where $\langle \cdot\,, \cdot \rangle$ denotes the standard scalar product. Finally, one can approximately obtain the spectrum of Lyapunov exponents of vibro-impact system (9) for N sufficiently large to be

$$\lambda_i \approx \frac{1}{N} \sum_{n=1}^{N} \ln \|m_i^{(n)}\|, \quad (i = 1, 2, 3, 4). \tag{42}$$

5. Numerical simulations

When the parameters have the values $\mu_k = 5, \mu_m = 2, \zeta = 0.05, f_2 = 0, \omega = 4, R = 0.8, \tau = \pi$ and $b = 0.1$, the time histories of the oscillators M_1 and M_2 with displacements x_1 and x_2 are shown in Figs. 3(a) and 3(b), respectively. Figures 3(c) and 3(d) are the phase portraits of the oscillators M_1 and M_2 and figure 3(e) shows the phase portrait in the x_1–x_2 plane. The test of the convergence of the iteration sequences of the spectrum of Lyapunov exponents is shown in Fig. 3(f). It is seen from Fig. 3(f) that there are four negative Lyapunov exponents (Here λ_1 and λ_2 are too close to be distinguished and so are λ_3 and λ_4), which confirms that it is a periodic attractor and consistent with the phase portrait. For this iteration sequence, 30000 iterations are taken of which the first 2000 iterations are omitted as the transient process.

When the parameters have the values $\mu_k = 4, \mu_m = 6, \zeta = 0.5, f_2 = 2, \omega = 1, R = 0.8, \tau = \pi$ and $b = 0.2$, the time histories of the oscillators M_1 and M_2 with displacements x_1 and x_2 are shown in Figs. 4(a) and 4(b), respectively. Figures 4(c) and 4(d) are the phase portraits of the oscillators M_1 and M_2 and figure 4(e) shows the phase portrait in the x_1–x_2 plane. The test of the convergence of the iteration sequences of the spectrum of Lyapunov exponents is shown in Fig. 4(f). It is seen from Fig. 4(f) that there are four negative Lyapunov exponents (where λ_2 and λ_3 are close enough), which confirms that it is also a periodic attractor and consistent with the phase portrait. For this iteration sequence, 15000 iterations are taken of which the first 2000 iterations are omitted as the transient process.

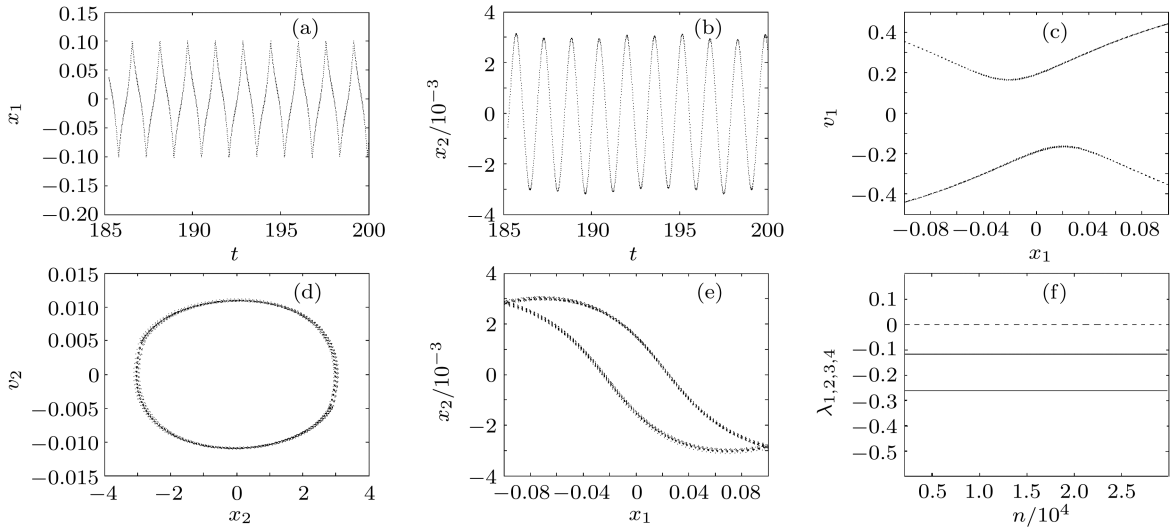


Fig. 3. Periodic attractor of the vibro-impact system. (a) Time history of the displacement of oscillator M_1, (b) time history of the displacement of oscillator M_2, (c) phase portrait of oscillator M_1, (d) phase portrait of oscillator M_2, (e) phase portrait in x_1–x_2 plane, (f) convergent sequence in the iteration process of the spectrum of Lyapunov exponents of the periodic attractor.

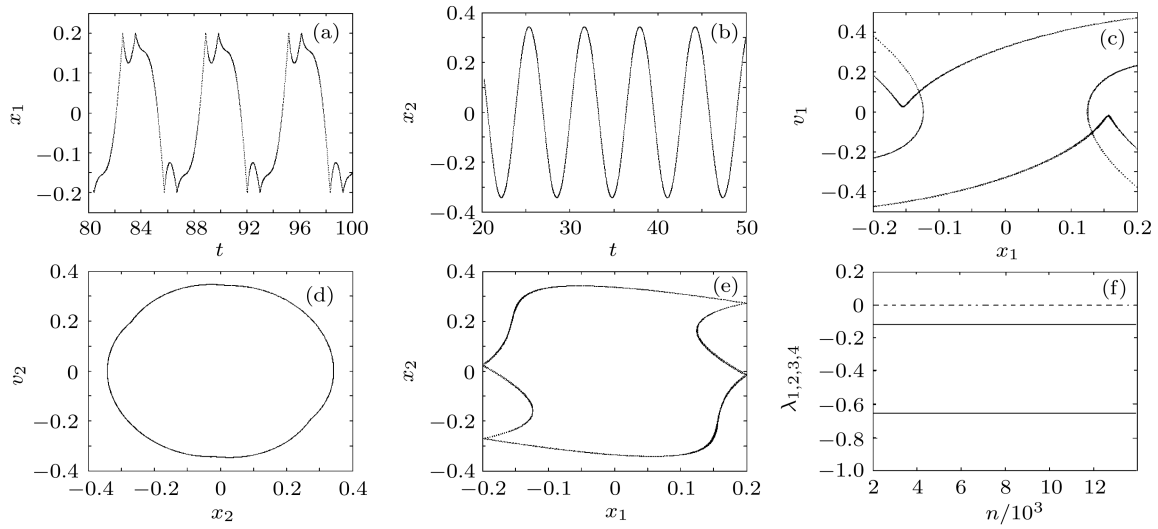


Fig. 4. The periodic attractor of the vibro-impact system. (a) Time history of the displacement of oscillator M_1, (b) time history of the displacement of oscillator M_2, (c) phase portrait of oscillator M_1, (d) phase portrait of oscillator M_2, (e) phase portrait in x_1–x_2 plane, (f) convergent sequence in the iteration process of the spectrum of Lyapunov exponents of the periodic attractor.

When the parameters have the values $\mu_k = 2, \mu_m = 2, \zeta = 0.5, f_2 = 5, \omega = 3, R = 0.8, \tau = \pi$ and $b = 0.2$, the time histories of the oscillators M_1 and M_2 with displacements x_1 and x_2 are shown in Figs. 5(a) and 5(b), respectively. Figures 5(c) and 5(d) are the phase portraits of the oscillators M_1 and M_2. The test of the convergence of the iteration sequences of the spectrum of Lyapunov exponents is shown in Fig. 5(e). It is seen from Fig. 5(e) that there are three negative Lyapunov exponents (where λ_2, λ_3 are close enough) and one positive Lyapunov exponent, which confirms that there is a chaotic attractor and it is consistent with the phase portrait of the system. For this iteration sequence, 25000 iterations are taken of which the first 5000 iterations are omitted as the transient process.

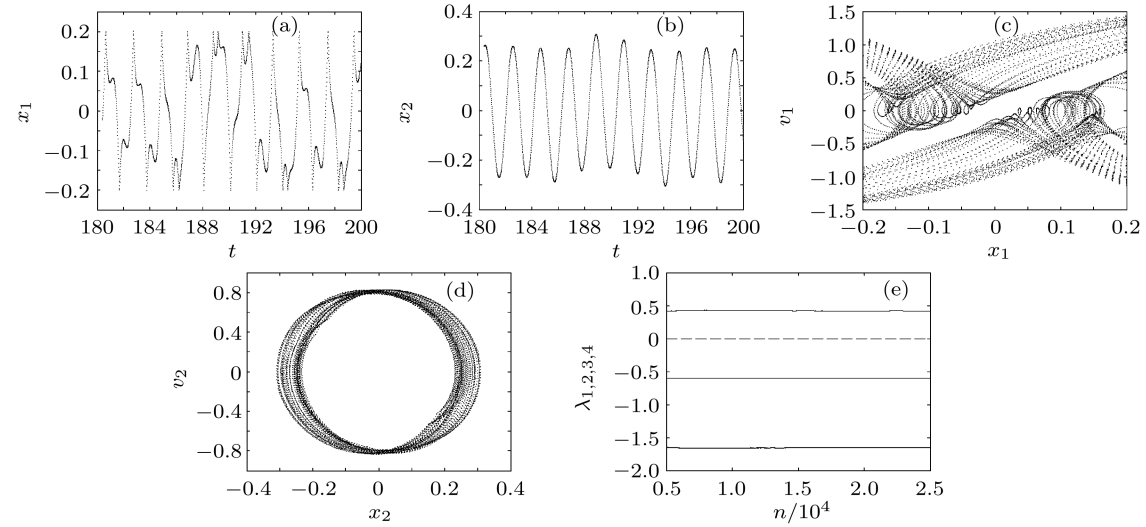


Fig. 5. Chaotic attractor of the vibro-impact system. (a) Time history of the displacement of oscillator M_1, (b) time history of the displacement of oscillator M_2, (c) phase portrait of oscillator M_1, (d) phase portrait of oscillator M_2, (e) convergent sequence in the iteration process of the spectrum of Lyapunov exponents of the chaotic attractor.

To show the correctness of our algorithm for a wide range of a control parameter, we plot a bifurcation diagram (Fig. 6(a)) and the corresponding largest Lyapunov exponent (Fig. 6(b)) with the parameters $\mu_k = 5, \mu_m = 2, \zeta = 0.05, f_2 = 0, R = 0.8, \tau = \pi, b =$ 0.15 and bifurcation parameter ω changing from 2 to 4. Here we use 8000 iterations for the exponent calculation, of which the first 3000 iterations are omitted as the transient process. In these figures, the increment of parameter ω is taken as 0.001. Obviously,

the attractor behaviours shown in bifurcation diagram can be determined by their corresponding largest Lyapunov exponent values. When the system encounters bifurcations, the corresponding largest Lyapunov exponents are equal to zero (Fig. 6(b)), for example, at $\omega = 2.008, 2.026, 2.066, 2.101, 2.214, 2.235, 2.45, 3.004$, etc.

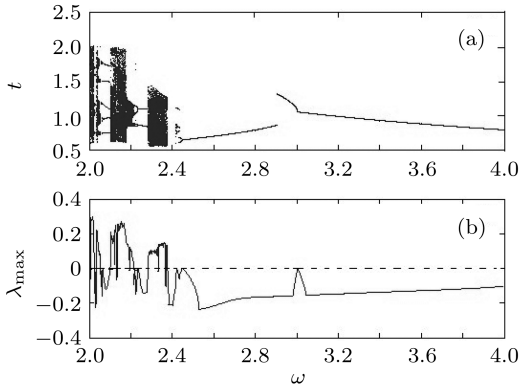


Fig. 6. Bifurcation diagram of the system and the largest Lyapunov exponent as parameter ω changes.

6. Conclusion

The calculation of the spectrum of Lyapunov exponents of a two-degree-of-freedom vibro-impact system having symmetrical rigid stops and subjected to periodic excitations is performed. With the local map, the Poincaré map method and the Gram–Schmidt orthogonalization and normalization method, we obtained the method of calculating the spectrum of Lyapunov exponents of a vibro-impact system with symmetrical rigid stops, which extends the application range of the method originating from Ref. [7]. Then the phase portraits of periodic and chaotic attractors for the discussed system and the corresponding convergence diagrams of the spectrum of Lyapunov exponents are shown via the numerical simulations. Furthermore, the bifurcation diagram of the system with respect to the bifurcation parameter ω and the corresponding largest Lyapunov exponents are given simultaneously.

References

[1] Benettin G, Galgani L, Giorgilli A and Strelcyn J M 1980 *Meccanica* **15** 9

[2] Benettin G, Galgani L, Giorgilli A and Strelcyn J M 1980 *Meccanica* **15** 21

[3] Wolf A, Swift J B, Swinney H L and Vastano J A 1985 *Physica* D **16** 285

[4] Müller P C 1995 *Chaos, Solitons and Fractals* **5** 1671

[5] De Souza S L T and Caldas I L 2004 *Chaos, Solitons and Fractals* **19** 569

[6] Nordmark A B 1991 *J. Sound Vib.* **145** 279

[7] Jin L, Lu Q S and Twizell E H 2006 *J. Sound Vib.* **298** 1019

[8] Luo G W, Ma L and Lü X H 2009 *Nonlinear Anal. Real.* **10** 756

[9] Yue Y and Xie J H 2009 *Phys. Lett.* A **373** 2041

[10] Stefanski A 2000 *Chaos, Solitons and Fractals* **11** 2443

[11] Liu W D, Ren K F, Meunier-Guttin-Cluzel S and Gouesbet G 2003 *Chin. Phys.* **12** 1366